UNIVERSITÄT AUGSBURG
Universitätsbibliothek

OPEN ACCESS
OPUS AUGSBURG

Aperiodically ordered nano-graphene on the quasicrystalline substrate

M. Maniraj, Lu Lyu, S. Mousavion, S. Becker, S. Emmerich, D. Jungkenn, D. L. Schlagel, T. A. Lograsso, S. R. Barman, S. Mathias, Benjamin Stadtmüller, M. Aeschlimann

Angaben zur Veröffentlichung / Publication details:

Maniraj, M., Lu Lyu, S. Mousavion, S. Becker, S. Emmerich, D. Jungkenn, D. L. Schlagel, et al. 2020. "Aperiodically ordered nano-graphene on the quasicrystalline substrate." *New Journal of Physics* 22 (9): 093056. https://doi.org/10.1088/1367-2630/abb342.

Nutzungsbedingungen / Terms of use:

CC BY 4.0

Dieses Dokument wird unter folgenden Bedingungen zur Verfügung gestellt: / This document is made available under these conditions:
CC-BY 4.0: Creative Commons: Namensnennung
Weitere Informationen finden Sie unter: / For more information see:
https://creativecommons.org/licenses/by/4.0/deed.de

New Journal of Physics
The open access journal at the forefront of physics

Deutsche Physikalische Gesellschaft DPG

IOP Institute of Physics

PAPER • OPEN ACCESS

Aperiodically ordered nano-graphene on the quasicrystalline substrate

To cite this article: M Maniraj *et al* 2020 *New J. Phys.* **22** 093056

View the article online for updates and enhancements.

You may also like

- The atomic structure of the threefold surface of the icosahedral Ag–In–Yb quasicrystal
C Cui, P J Nugent, M Shimoda et al.
- Metallic–covalent bonding conversion and thermoelectric properties of Al-based icosahedral quasicrystals and approximants
Yoshiki Takagiwa and Kaoru Kimura
- Surfaces of Al-based complex metallic alloys: atomic structure, thin film growth and reactivity
Julian Ledieu, Émilie Gaudry and Vincent Fournée

This content was downloaded from IP address 137.250.100.44 on 14/05/2024 at 15:25

New Journal of Physics
The open access journal at the forefront of physics

Deutsche Physikalische Gesellschaft DPG
IOP Institute of Physics

Published in partnership with: Deutsche Physikalische Gesellschaft and the Institute of Physics

OPEN ACCESS

RECEIVED
29 June 2020

REVISED
20 August 2020

ACCEPTED FOR PUBLICATION
27 August 2020

PUBLISHED
18 September 2020

Original content from this work may be used under the terms of the Creative Commons Attribution 4.0 licence.

Any further distribution of this work must maintain attribution to the author(s) and the title of the work, journal citation and DOI.

PAPER

Aperiodically ordered nano-graphene on the quasicrystalline substrate

M Maniraj[1,6], L Lyu[1], S Mousavion[1], S Becker[1,2], S Emmerich[1], D Jungkenn[1], D L Schlagel[3], T A Lograsso[3], S R Barman[4], S Mathias[5], B Stadtmüller[1] and M Aeschlimann[1]

[1] Department of Physics and Research Center OPTIMAS, University of Kaiserslautern, 67663 Kaiserslautern, Germany
[2] Department of Chemistry, University of Kaiserslautern, 67663 Kaiserslautern, Germany
[3] Division of Materials Sciences and Engineering, Ames Laboratory, Ames Iowa 500011-3020, United States of America
[4] UGC-DAE Consortium for Scientific Research, Khandwa Road, Indore 452001, Madhya Pradesh, India
[5] I. Physikalisches Institut, Georg-August-Universität Göttingen, Friedrich-Hund-Platz 1, 37077 Göttingen, Germany
[6] Author to whom any correspondence should be addressed.

E-mail: mr.maniraj@gmail.com

Keywords: quasicrystal, Penrose tiling, graphene, interface state, electronic structure, photoemission, intermetallic alloy

Abstract

Designing exotic structures in low dimensions is key in today's quest to tailor novel quantum states in materials with unique symmetries. Particularly intriguing materials in this regard are low dimensional aperiodic structures with non-conventional symmetries that are otherwise forbidden in translation symmetric crystals. In our work, we focus on the link between the structural and electronic properties of aperiodically ordered aromatic molecules on a quasicrystalline surface, which has largely been neglected so far. As an exemplary case, we investigate the self-assembly and the interfacial electronic properties of the nano-graphene-like molecule coronene on the bulk truncated icosahedral (i) Al–Pd–Mn quasicrystalline surface using multiple surface sensitive techniques. We find an aperiodically ordered coronene monolayer (ML) film on the i-Al–Pd–Mn surface that is characterized by the same local motifs of the P1 Penrose tiling model as the bare i-Al–Pd–Mn surface. The electronic valence band structure of the coronene/i-Al–Pd–Mn system is characterized by the pseudogap of the bare i-Al–Pd–Mn, which persists the adsorption of coronene confirming the quasiperiodic nature of the interface. In addition, we find a newly formed interface state of partial molecular character that suggests an at least partial chemical interaction between the molecule and the quasicrystalline surface. We propose that this partial chemical molecule–surface interaction is responsible for imprinting the quasicrystalline order of the surface onto the molecular film.

1. Introduction

Quasicrystals are one the most interesting discoveries in condensed matter physics of the last century. They are characterized by an ordered aperiodic arrangement of atoms and exhibit rotational symmetries and diffraction signatures that are forbidden in ordinary crystals [1–3], such as five-fold (f), 8f, 10f, and 12f rotational symmetry. The discovery of quasicrystals has not only altered our understanding and classification of crystalline materials, but also started the quest to uncover quasicrystalline order in different classes of condensed matter systems.

Quasicrystalline order can exist in a variety of bulk materials ranging from intermetallic alloys [2], natural rock [4, 5], oxides [6], to soft condensed matter [7]. However, quasicrystalline order is not limited to bulk materials, but has recently also been observed in crystalline two-dimensional bilayer systems [8, 9] and adsorbate layers on quasicrystalline surfaces [10–21]. Interestingly, the quasicrystalline order of low-dimensional systems is not necessarily an intrinsic property of the adsorbate systems and the 2D honeycomb materials themselves, but arises due to the interaction between the constituents forming the low

© 2020 The Author(s). Published by IOP Publishing Ltd on behalf of the Institute of Physics and Deutsche Physikalische Gesellschaft

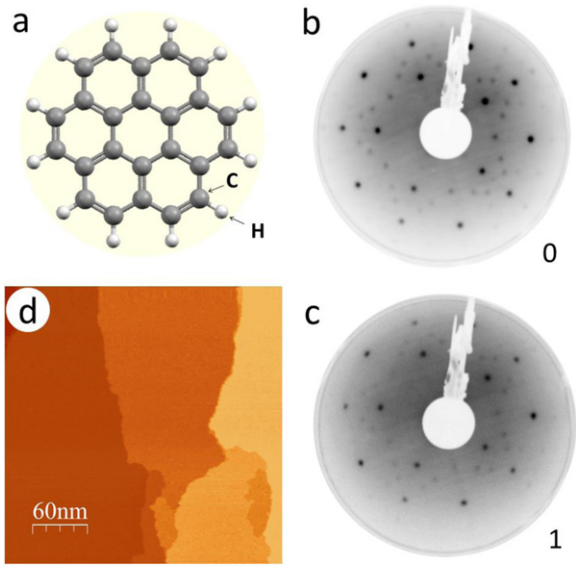

Figure 1. (a) Ball and stick model of coronene molecule. H (white) and C (gray) indicate hydrogen and carbon atoms, respectively. LEED pattern of the (b) bare i-Al–Pd–Mn quasicrystal surface and (c) the coronene covered i-Al–Pd–Mn surface. The electron energy and substrate temperature are 78 eV and 300 K, respectively. 0 and 1 in (b) and (c) indicate the coverage of coronene in units of ML on i-Al–Pd–Mn quasicrystalline surface. (d) Large area overview STM image of a ML of coronene adsorbed on i-Al–Pd–Mn surface measured at 100 K with tunneling parameter of −2.4 V and 200 pA.

dimensional (hybrid) material. For instance, two interacting sheets of crystalline graphene exhibit a quasiperiodic diffraction pattern with multiple Dirac cones when twisted by 30° [8, 9]. On the other hand, molecular adsorbates such as fullerene, pentacene, and corannulene reveal aperiodic order on quasicrystal substrates [22–26] despite their typically long-range ordered crystalline superstructures on noble metal surfaces [27–30]. This surface-induced templating of molecular materials is particularly interesting, since it allows one to tailor and functionalize quasiperiodic molecular 2D structures on surfaces by controlling the interaction across the molecule-quasicrystalline interfaces. This could, on the long term, offer the intriguing opportunity to design and study quantum states in low-dimensions in the limits between long-range crystalline order and disordered amorphous. However, the realization of this goal is still hindered by our limited understanding of the phenomena occurring at interfaces between organic molecules and quasicrystalline surfaces. This is particularly true for the electronic band structure at such interfaces, which has largely been neglected so far.

In our work, we therefore focus on the link between the structural and electronic properties of the nano-graphene-like molecule coronene ($C_{24}H_{12}$) grown on an infinitely aperiodic bulk truncated quasicrystal surface of icosahedral (i)-Al–Pd–Mn. Coronene is a six-fold symmetric molecule consisting of seven aromatic benzene rings arranged in a honeycomb-like structure as shown in the ball and stick model in figure 1(a). As a result of this graphene-like structure, it resembles many of the electronic properties of a nanometer sized graphene sheet. For instance, the positions of the coronene valence orbitals in energy and momentum space follow the dispersion of the graphene π-band [31–34] and interface states of graphene on noble metals possess the signature of the Dirac cone-like state [35]. Due to these intriguing properties, coronene is an interesting choice to study the influence of a quasiperiodic template on the structure and electronic interface properties of such a highly symmetric adsorbate system.

In our experimental study, we combine low energy electron diffraction (LEED), scanning tunneling microcopy (STM) and angle resolved photoelectron spectroscopy (ARPES) to study the geometric and electronic properties of the coronene/i-Al–Pd–Mn interface. First of all, we are able to confirm the formation of an aperiodic coronene structure on the surface of the i-Al–Pd–Mn quasicrystal. The local arrangement of the coronene overlayer can be explained by the P1 Penrose tiling, where the molecules decorate only the positions of the pentagonal tiles. Our photoemission study reveals the electronic surface band structure of the quasicrystal after the adsorption of coronene. The spectroscopic signature of the quasicrystalline surface, the pseudogap, persists after coronene adsorption. In contrary, the 5*f* symmetric emission pattern of the i-Al–Pd–Mn valence bands are superimposed by a ring-like emission pattern of the highest occupied molecular orbital (HOMO) of coronene molecules. Most interestingly, we find a small spectroscopic intensity of an adsorption-induced interface state. We propose that this interface state is the

spectroscopic signature of the (at least partial) chemical molecule–surface interaction that is responsible for the surface-mediated quasicrystalline order of the coronene layer.

2. Method

Our LEED, STM, and ARPES experiments were carried out at different ultrahigh vacuum chambers with base pressures better than 1×10^{-10} mbar. LEED pattern were recorded using a 4 grid rear view instrument at 300 K. All STM images were recorded at 100 K (using liquid N_2 cooling) in constant current mode using an Au tip and *in situ* sputtered and annealed W tip as in our previous work [36]. The STM images were processed with the Nanotec Electronica WSxM software [37] and Gwyddion [38]. The ARPES study was performed using non-polarized monochromatized He I_α (21.22 eV) light (ScientaVUV5k) with a 150 mm hemispherical analyzer (Specs PHOIBOS 150). The total energy and angular resolutions are better than 100 meV and 0.3°, respectively. To obtain the k_x–k_y map we measured the photocurrent $I(E_B, \theta, \varphi)$ for a wide range of binding energies (E_B) by sweeping the azimuth angle (φ) over a range of 224° in step of 2° and the polar angle (θ) in steps of 15°. The data has been converted from $I(E_B, \theta, \varphi)$ to $I(E_B, k_x, k_y)$ using

$$k_{\parallel,x} = (\hbar^2/2m_e)\sin(\theta)\cos(\phi)\sqrt{}(h\nu - E_B - \phi)$$

$$k_{\parallel,y} = (\hbar^2/2m_e)\sin(\theta)\cos(\phi)\sqrt{}(h\nu - E_B - \phi)$$

where $\hbar$, m_e, ϕ and $h\nu$ are the Planck's constant, the free electron mass, the work function of the sample, and the photon energy, respectively. All photoemission measurements were performed at room temperature.

The quasicrystalline surface was prepared from a single grain of the i-$Al_{69.4}Pd_{20.8}Mn_{9.8}$ bulk quasicrystal cut perpendicular to its 5*f* axis. The surface was first polished *ex situ* using diamond paste with particle sizes down to 0.25 microns. In UHV, the sample was cleaned by repeated cycles of Ar ion sputtering using 1.5 keV for 1 hour, followed by sample annealing up to 930 K for 3 hours [20, 21]. The quality of surface morphology, the defect density and the quasicrystalline order of the surface were inspected by large-scale STM images and LEED. The coronene molecules were evaporated onto the clean surface at room temperature using a commercial Knudsen cell evaporator (Kentax GmbH) at a sublimation temperature of 400 K. In our work, we investigate a nearly closed layer of flat lying coronene molecules on the i-Al–Pd–Mn quasicrystal surface. This coverage is referred to as 1 monolayer (ML).

3. Results and discussion

We begin the discussion of our experimental findings with the structural characterization of the coronene ML film on the quasicrystal surface. In figures 1(b) and (c), we compare LEED patterns of the i-Al–Pd–Mn surface prior and after the adsorption of one ML of coronene. The LEED pattern remains identical after the adsorption of coronene, with only marginal changes in the relative intensity of the diffraction spots with respect to the background signal. This indicates a pseudomorphic growth and an aperiodic order of coronene on the i-Al–Pd–Mn surface, similar to previous findings for inorganic [10–12, 20, 21, 39] and organic adsorbates [22–24] on quasicrystal surfaces.

In figure 1(d), a large area overview STM image is presented which illustrates the smooth and uniform growth of coronene over multiple terraces. The absence of molecular 3D islands clearly indicates the dominant role of the molecule–surface interaction in comparison to the intermolecular coupling. The local arrangement of coronene on i-Al–Pd–Mn quasicrystal surface can be deduced from the STM data in figure 2. The molecular arrangement itself is demonstrated in the STM image with intermolecular resolution in figure 2(a) ($T_{\text{sample}} = 100$ K). The coronene molecules appear as bright point-like features which form a homogeneous overlayer over the entire surface. The typical size of this feature is 1 nm [40–42]. Importantly, there is no translational symmetry between the coronene molecules at any given location on the sample surface. This is consistent with the fast Fourier transform (FFT) of the STM in figure 2(b), which reveals a clear 10*f* rotational symmetry. It is important to note that the FFT only reveals the symmetry of the first layer, which, in our case, is the molecular layer. Thus, the missing translational symmetry in real space of the coronene molecules and its 10*f* rotational symmetry clearly proves the formation of an aperiodic order of the 2D coronene overlayer. Interestingly, the 10*f* symmetry of the molecular overlayer also follows the 10*f* symmetry (including mirror symmetry) of the i-Al–Pd–Mn quasicrystal surface. This suggests a direct influence of the surface structure on the quasiperiodic arrangement of the molecular overlayer, in agreement with our LEED analysis.

The quasicrystalline order of the coronene layer is not only reflected in the FFT of the STM image, but also directly visible in the STM image in figure 2(a). Upon close inspection, it becomes clear that the

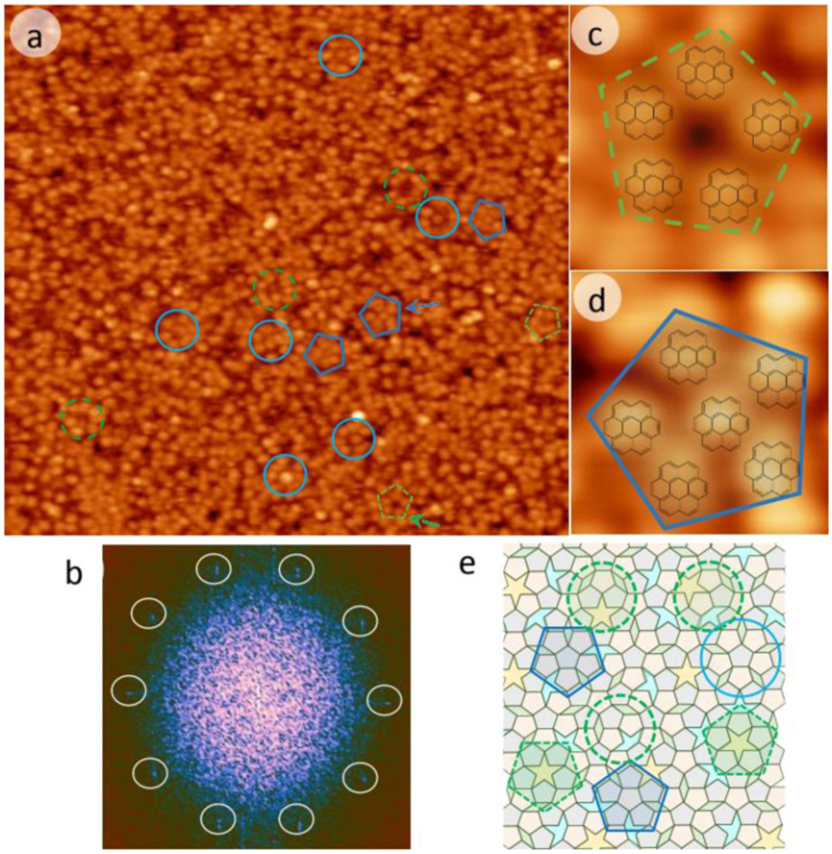

Figure 2. (a) Molecular-resolved STM image (70 nm × 70 nm) of the coronene film on the i-Al–Pd–Mn surface recorded at 100 K ($V_{bias} = -1.6$ V, $I = 70$ pA). The filled (empty) pentagonal motifs are marked by blue-continuous (green-dashed) pentagons. Circular motifs with filled (empty) center portion are shown by blue-continues (green-dashed) circles. (b) The fast Fourier transformation of the STM image shown in (a). The ten spots in the FFT are marked by yellow circles. (c) and (d) show enlarged view of the two types of pentagon motifs (4.8 nm × 4.8 nm) marked by arrows of identical color in (a). Color scale range for each individual image is optimized such that as many features as possible are readily visible. Dark and bright indicates the lowest and highest height, respectively. Overlaid are arbitrarily oriented coronene molecules as a guide to the eye. (e) Model of the τ-scaled P1 Penrose tiling (edge length of 1.26 nm) formed by the combination of star, boat, pentagon and thin rhombus. The local isomorphism formed by the finite region is marked by circles with different color. Pentagons with centers with a star (solid-black) and a pentagon (dashed-blue) are highlighted in different colors. Size is 22.8 nm × 24.8 nm.

coronene molecules form pentagonal motifs that are commonly associated with the quasicrystalline order of icosahedral quasicrystalline surfaces [11, 12, 16, 19]. Interestingly, we observe two types of pentagon motifs consisting of coronene molecules (figures 2(c) and (d)). One pentagon motif exhibits a void in its center position (empty-center pentagon motif, figure 2(c)), the other one reveals an additional coronene molecule at its center (filled-center pentagon motif, figure 2(d)). We have marked these pentagon motifs in figures 2(a)–(d) in identical colors.

In analogy to the pentagons, we further identified empty-center and filled-center circular motifs. They are formed by a set of coronene molecules arranged in a ring-like structure surrounding either a void (missing coronene molecule, empty-center circular motif, dashed circle) or an additional coronene molecule (filled-center circular motif, solid circle) as shown in figure 2(a). The empty-center circular-motifs typically consist of 6 to 8 molecules with a diameter of about 6 nm. The filled-center circular-motifs are formed by 8 to 9 molecules located on the ring and one coronene molecule located at the center. In all cases, the average intermolecular distance between neighboring molecules forming pentagon and circular motifs is 1.7 ± 0.1 nm.

To understand the arrangement of coronene molecules in pentagonal and circular motifs, we turn to the P1 Penrose tiling [43]. The P1 Penrose tiling is the most simple mathematical model to explain quasicrystalline order in 2D space for a 5*f* symmetric structure. This tiling model has also been successfully applied to describe the atomic structure of the bare i-Al–Pd–Mn quasicrystal surface as confirmed by DFT calculations [16, 19, 44, 45] and has therefore been chosen as our model.

The P1 Penrose tiling consists of four fundamental units: *star*, *boat*, *pentagon* and *thin rhombus*. Using specific matching rules [43], this model allows one to fill the entire 2D plain with an aperiodic and 5*f* symmetric structure with these fundamental units. An exemplary arrangement of these units in the 2D

plane is shown in figure 2(e) for a small part of the surface. We use this model and its characteristic motifs to identify characteristic signatures of the quasicrystalline order of the molecular layer in our experiment.

In this model, we can primarily identify two different types of pentagon motifs, namely the star-centered pentagon (SCP, dashed-green) and the pentagon-centered pentagon (PCP, continuous-blue) motifs. The SCP consists of five pentagon tile units, while the PCP consists of six pentagon tile units. These different pentagon motifs of the P1 Penrose tiling can directly explain the two different pentagon-like arrangements of coronene molecules on the surface assuming that only one coronene molecule adsorbs on one pentagonal tile. For the PCP motif, five coronene molecules adsorb on the outer pentagon tiles forming a five-fold symmetric pentagon-like arrangement. An additional coronene molecule can adsorb on the pentagon tile in the center of the PCP motif resulting in the pentagon-like arrangement of six coronene molecules observed in the experiment. For the SCP motifs, the center position is occupied by the star-like tile. The latter tile seems to be a less preferred adsorption position (due to the size/shape mismatch between the tile and coronene molecuels) compared to the pentagon tile and hence cannot host an additional coronene molecule leaving a void in the center of the pentagon-like coronene arrangement. The existence of both pentagon-like motifs in the experiment again confirms the quasicrystalline order of the coronene overlayer that is inherent in the P1 Penrose tiling model.

Next, we discuss the origin of circular motifs of coronene molecules observed in figure 2(a) (continuous-blue and dashed-green circles) using the P1 Penrose tiling model. These motifs can be qualitatively understood by the local isomorphism [3, 46] of the quasiperiodic structure, i.e. any specific area of interest with a specific set of basic tiles can also be found in the other neighboring locations. In a quasiperiodic 2D structure, the 2D space is filled with an aperiodic arrangement of certain motifs such as the PCP and SCP motifs discussed above. Due to the aperiodic arrangement, the areas between these well recognizable motifs is never identical and must be filled with different arrangements of fundamental tiles. In most simple cases, these arbitrary arrangement of tiles results in the formation of circular motifs, as highlighted for instance with continuous-blue colored circle in figure 2(e), where 10 pentagons are joined together enclosing a circular motif. Other circular motifs are indicated by dashed-green colored rings in figure 2(e). Circular motifs are hence the simplest local isomorphism that can be identified within the P1 Penrose tiling model. To match the theoretically expected circular motifs to our experimental findings, we again have to assume that coronene molecules preferentially occupy the pentagon tiles, and not the star, rhombus and boat tiles. In this way, it is possible to correlate the experimentally observed filled or empty-center circular motifs with the P1 Penrose model for an aperiodic surface. The pentagon selective adsorption of coronene further explains the many voids in the coronene film on the i-Al–Pd–Mn surface. This high density of voids is also responsible for the rather irregular appearance of the spatial arrangement of coronene molecules in our large scale STM image in figure 2(a).

Although the P1 Penrose tiling model can qualitatively describe the pentagonal and circular coronene motifs on the surface, it cannot directly explain the experimentally observed intermolecular distance of 1.7 nm. In particular, the intermolecular distance is significantly larger than the characteristic edge length of the fundamental P1 Penrose tiling model (0.78 nm [16, 44]) used for the bare i-Al–Pd–Mn surface and of the τ-scaled P1 tiling model (1.26 nm, $\tau = 1.618$) used to model atomic adsorbates such as Pb. On the other hand, the intermolecular distance is smaller compared to the edge length of the τ^2-scaled P1 tiling model (2.03 nm). This conundrum can only be resolved when considering the Gaussian-like distribution function of the intermolecular distance between neighboring coronene molecules, which exhibits a rather large full width at half maximum (FWHM) of 0.7 nm. Such a large FWHM points to a strong variation of the intermolecular distance, at least between the limits of the characteristic edge lengths of the τ- and τ^2-scaled P1 tiling model. Based on this variation of the intermolecular distance, we must conclude that the characteristic and well-defined edge length of the surface tiles cannot determine the adsorption position of coronene on the i-Al–Pd–Mn surface. Instead, we propose that the coronene position is defined by the local atomic structure of the surface underneath the molecules. Only such a site-specific molecule–surface interaction can account for the large variation of the experimentally observed intermolecular distance as the local atomic surface structure differs for each pentagonal motif of the i-Al–Pd–Mn surface [16].

Overall, our structural characterization of the coronene film on the i-Al–Pd–Mn surface reveals clear indications of a quasiperiodic arrangement of the molecular film. In particular, modeling the local molecular motifs in the framework of the P1 Penrose tiling allows us to identify the pentagonal sites as the favorable adsorption position of coronene on the i-Al–Pd–Mn surface. This clearly indicates that the structure formation of the coronene overlayer is determined by the molecule–surface interaction and the surface potential landscape of the quasicrystalline surface.

We now turn to the electronic properties of the quasicrystalline molecular film on the quasicrystal surface. An overview of the electronic valence band structure is shown in the valence band spectra measured at normal emission geometry in figure 3(a). The data for the bare i-Al–Pd–Mn surface and 1 ML

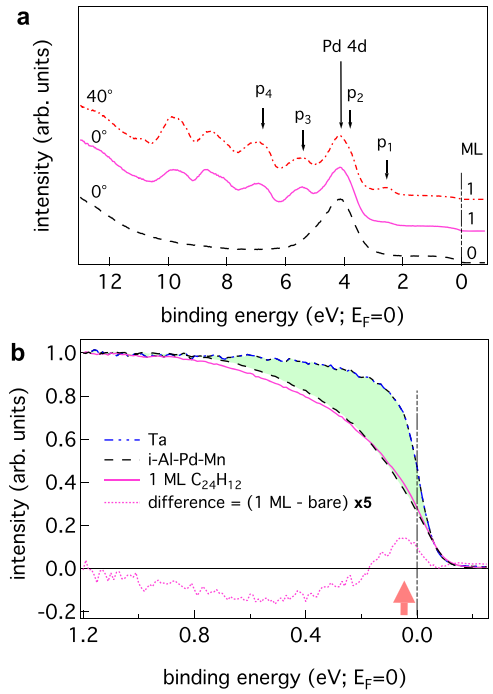

Figure 3. (a) Valence band spectra measured using He I_α (21.2 eV) light at normal emission geometry for the bare and 1 ML of coronene covered i-Al–Pd–Mn quasicrystal surface. The spectrum of the molecular film shown by a dotted line in (a) was recorded in 40° off-normal emission geometry. The arrows in (a) indicate the first four molecular levels and the Pd 4*d* related peak position. 0 and 1 in (a) mark the coverage of coronene in units of ML on the i-Al–Pd–Mn quasicrystalline surface. (b) Photoemission spectrum of the near Fermi edge region of the bare and 1 ML of coronene covered i-Al–Pd–Mn quasicrystal surfaces measured in normal emission geometry. The pseudogap is highlighted by the green shaded area. The 5 × enlarged difference spectrum obtained by subtracting the bare i-Al–Pd–Mn surface spectrum from the one of the 1 ML film coronene is shown at the bottom of (b). The spectra in (b) are normalized to unity at around 1.2 eV, where no influence of the pseudogap is expected. The arrow in the vicinity of the Fermi level in (b) indicates the adsorption-induced interface state.

of coronene on the i-Al–Pd–Mn surface are shown as dashed black and continuous pink line, respectively. For the bare i-Al–Pd–Mn surface, a peak originating from the Pd 4*d* states is visible at a binding energy of $E_B \approx 4.1$ eV [47–49]. For the coronene covered surface, the signature of the HOMO of coronene appears at $E_B \approx 2.5$ eV (labeled as p_1). p_1 is more clearly visible in the spectrum recorded at 40° off-normal emission (dotted red line). The enhanced intensity of the molecular features in comparison to substrate states at larger emission angles is due to the enhanced surface sensitivity at grazing incidence and the strong angular dependence of the photoemission intensity distribution of molecular materials [30, 31, 50–52]. The HOMO signature is the first peak of a series of molecular features that are separated in energy by nearly 1.5 eV [53]. p_2 is the signature of a subsequent molecular orbital (HOMO−1) with lower binding energy and appears as a shoulder of the Pd 4*d* related peak at $E_B \approx 3.8$ eV.

We have further investigated the electronic structure around the Fermi level. This part of the band structure exhibits the most distinct electronic signature of quasicrystal materials: a reduced density of states (DOS) known as pseudogap [2, 21, 47–49]. The existence of a pseudogap is regarded as a necessary and essential spectroscopic signature for quasicrystals. Pseudogaps are observed for a variety of different quasicrystal surfaces with various pseudogap values depending on the material and the probing depth of the employed spectroscopic technique [12, 21, 48, 49]. In most cases, the pseudogap of a particular surface remains intact or even becomes more pronounced after the adsorption of inorganic materials forming aperiodically ordered overlayers on quasicrystalline substrates [12, 17, 20].

In our case, we investigate the nature of the pseudogap for a ML film of coronene, which is shown in figure 3(b). For comparison, the spectrum of the metallic Ta sample plate is included as a blue dotted line. The suppression of DOS for bare i-Al–Pd–Mn around the Fermi energy compared to the metal Ta is indicated by the green shaded area. The latter highlights the pseudogap. The overall spectral shape of the pseudogap of the i-Al–Pd–Mn surface remains similar after the adsorption of one ML of coronene. Small changes of the spectral lineshape are better visible in the difference curve obtained by subtracting the bare i-Al–Pd–Mn surface spectrum from the 1 ML coronene spectrum. The difference curve is magnified by a factor of five and is included at the bottom of figure 3(b). It clearly shows that the pseudogap persists after the adsorption of coronene, thus confirming the quasicrystalline nature of the coronene/i-Al–Pd–Mn interface.

Most interestingly, we find another peak-like spectral feature in the difference curve at $E_B \approx 50$ meV, indicated by an arrow in figure 3(b). A comparable spectroscopic feature has never been observed for any inorganic adsorbates on a quasicrystal surface, for instance, K and Sn covered i-Al–Pd–Mn surfaces [21, 39, 54]. In contrast, the emergence of new states close to the Fermi energy is frequently observed for molecular adsorbates on noble metals [55–61]. They are the result of a charge redistribution between the surface and the adsorbate layer which leads to an, at least, partial occupation of the otherwise lowest unoccupied molecular orbital (LUMO) of the adsorbates. These LUMO-derived states can be regarded as a spectroscopic signature of a (at least) partial chemical interaction between the molecule and the surface. In analogy, we propose that this new state is the signature of the chemical interaction between coronene and the i-Al–Pd–Mn surface. The small intensity of this peak is hence a result of the extremely small charge transfer between the molecule and the surface, possibly due to the low density of substrate states in the pseudogap. Since this tiny peak appears due to the presence of the organic adsorbate, we refer to this peak as adsorption-induced interface state.

To gain further insights into electronic properties of the coronene/i-Al–Pd–Mn interface, we recorded momentum-resolved photoemission data throughout the entire valence band structure for the bare and coronene covered i-Al–Pd–Mn surface. Selected constant binding energy (CBE) maps for the bare and coronene covered i-Al–Pd–Mn surface are shown in figure 4.

We first focus on the CBE maps of the bare i-Al–Pd–Mn surface, since momentum-resolved photoemission data have not been reported so far for any 3D icosahedral quasicrystal surface. The Fermi surface map ($E_B = 0$ eV) of the bare i-Al–Pd–Mn surface (figure 4(a)) reveals an overall 5*f* symmetric photoemission pattern with distinct maxima distributed on a circle with a radius ($R_{|\mathbf{k}|}$) ≈ 0.9 Å^{-1}. In particular, we find four elliptical emission features (marked by black ellipses in figure 4(a)) in the measured momentum space range that are separated from each other by 72°. The positions of these emission maxima in momentum space hence match very well with the four vertexes of a pentagon marked in figure 4(a). Note that no symmetrization procedure was applied to these photoemission data. Therefore, these data provide unambiguous evidence for the existence of a 5*f* symmetric emission pattern that is characteristic for a quasicrystal in momentum space. The outlined momentum space emission features appear as ellipses and not circles. This is caused by an intrinsic effect within the photoemission tomography framework as shown in figure 4(g). In addition, the elliptic effect is enhanced due to an asymmetric angular resolution in the azimuthal direction compared to the radial direction.

In addition, we observe two sets of systematically modulated intensities for larger $R_{|\mathbf{k}|} \approx 1.4$ Å^{-1}, as shown by the dashed (weak in intensity) and continuous (strong in intensity) red colored ellipses in figure 4(a). These ellipses on the outer ring are separated by about 36° and thus show a 10*f* rotational symmetry. Similar, the CBE maps at larger binding energies of about 2.5 eV (figure 4(b)) and 4 eV (figure 4(c)) also reveal well-defined emission features in momentum space forming a 5*f* symmetric emission pattern as marked by ellipses. These findings are again a clear spectroscopic confirmation that the energy and momentum distributions of the electrons follow in the structural symmetry of the quasicrystal itself.

The CBE maps at these selected energies change significantly upon the adsorption of coronene on the i-Al–Pd–Mn surface (figures 4(d)–(f)). The photoemission signals from the substrate states are smeared out and attenuated due to the formation of the molecular layer. In fact, the 5*f* symmetric emission pattern is only visible in the CBE map at $E_B = 4$ eV (figure 4(f)), which originates from the Pd 4*d* states of the substrate. The CBE maps at $E_B = 2.5$ eV and 0 eV are attributed to the spectroscopic signatures of the coronene HOMO and the adsorption induced interface state, respectively. The CBE map of the coronene HOMO consists of the concentric ring-like emission features with marginal azimuthal intensity modulations in momentum space. The inner ring-like feature at $R_{|\mathbf{k}|,\,1} \approx 1$ Å^{-1} can also be observed as a background signal in the corresponding CBE map of the bare surface and is hence attributed to a residual photoemission signal of substrate states. In contrast, the second ring-like features at $R_{|\mathbf{k}|,\,2} \approx 1.5$ Å^{-1} has not been observed for the bare surface and hence represents the photoemission signal of the coronene HOMO (dashed line in figure 4(e)). To support this assignment, we have calculated the photoemission signal of the coronene HOMO level using the photoemission tomography formalism [50, 62]. The photoemission pattern calculated for an isolated molecule in a single orientation is shown in figure 4(g). It consists of six well-defined maxima at a distance of $R_{|\mathbf{k}|,\,\mathrm{HOMO}} \approx 1.5$ Å^{-1} from the center of the surface Brillouin zone [31]. The quasiperiodic lateral order of the molecular adsorbates on the surface coincides with the existence of different azimuthal molecular orientations according to the 5*f* symmetry of the surface. These different orientations are caused by different rotational domains on the surface and/or by structurally inequivalent molecules within one domain on the surface. When combining the 5*f* symmetry of the quasicrystalline surface with the six-fold symmetric emission pattern of a single coronene molecule, we obtain the molecular emission pattern as shown in figure 4(h) (dashed line). Every structure is smeared

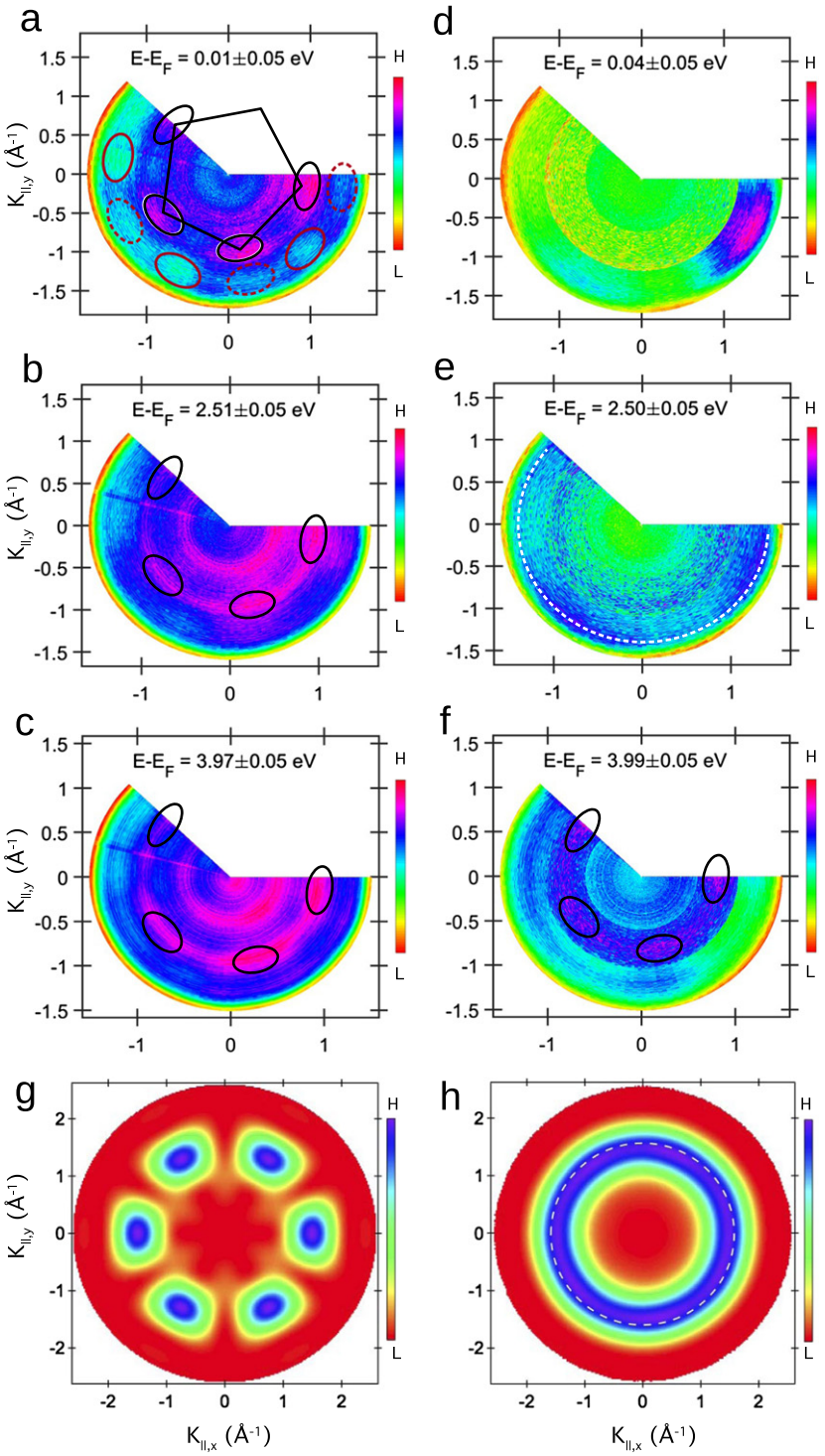

Figure 4. Selected CBE momentum distribution maps of ((a)–(c)) the bare i-Al–Pd–Mn quasicrystal surface and ((d)–(f)) the 1 ML coronene film on the i-Al–Pd–Mn quasicrystalline surface. (g) Predicted momentum space emission pattern for the coronene HOMO for a single azimuthal orientation of coronene. The emission characteristics were simulated using the photoemission tomography framework. Considering additionally the 5*f* symmetry of the quasicrystal surface results in the emission pattern of the coronene HOMO in (h). Ellipses, circles, and pentagon shapes highlight the 5*f* symmetry of photoemission intensity distribution. The binding energy of each constant energy map is included at the top of each panel. Error value represents the energy range used for averaging. Color scale range for each individual image is optimized such that as many features as possible are readily visible. Note the different axis and color scales of the different panels. Dashed line in (e) and (h) marks the ring like feature, guided to eye.

out due to the large FWHM of the emission maxima of the single coronene molecules in momentum space, resulting in a homogeneous ring-like emission feature with $R_{|\mathbf{k}|,\,\mathrm{HOMO}} \approx 1.5$ Å^{-1}. This consideration resembles the overall emission characteristics of the CBE map at $E_B = 2.4$ eV and hence supports our assignment of this spectroscopic feature to the HOMO of coronene on the i-Al–Pd–Mn quasicrystal surface.

Similar, the CBE map of the new adsorption induced interface state at $E_B = 0$ eV only reveals a ring-like emission feature with an azimuthal intensity modulation at $R_{|\mathbf{k}|} \approx 1.3$ Å^{-1}. Such an almost ring-like emission pattern is consistent with a molecular state of flat molecules adsorbed on a 5*f* symmetric surface as discussed above in detail for the coronene HOMO (see figure 4(h)). Hence, this finding suggests an at least partial molecular character of the adsorption induced interface state as supported by the difference spectrum in figure 3(b). Importantly, the azimuthal intensity modulation visible in figure 4(d) cannot be explained by a simple model considering only isolated, non-interaction coronene molecules. We propose that this strong intensity modulation can be the signature of the molecule–surface interaction of the planar coronene molecule on the quasicrystalline surface.

4. Conclusion

In conclusion, we have investigated the structure formation and the electronic interfacial properties of the prototypical aromatic molecule coronene on the quasicrystalline i-Al–Pd–Mn surface. Combining LEED and STM, we are able to demonstrate that coronene follows the quasicrystalline order of the i-Al–Pd–Mn surface: the diffraction pattern reveals the characteristic 5*f* symmetry of the quasicrystal surface while STM uncovers the lack of any translational symmetry of the molecular overlayer. Moreover, the local aperiodic arrangement of the coronene molecules on i-Al–Pd–Mn can be modeled by the P1 Penrose tiling. This enables us to identify two types of pentagon and circular motifs as the dominant building blocks of the quasiperiodic order, in agreement with the tiling model for the bare i-Al–Pd–Mn surface. Similarly, the electronic valence band structure of the coronene ML film on i-Al–Pd–Mn reveals clear signatures of an interface with quasiperiodic order. The pseudogap of bare i-Al–Pd–Mn surface persists even after the adsorption of one layer of coronene providing clear evidence for the quasicrystalline nature of the interface. Even more interestingly, the spectroscopic signal within the pseudogap exhibits an adsorption induced interface state in the vicinity of the Fermi level that reveals at least partial molecular character. We attribute this new interface state to an at least partial chemical interaction between the quasicrystalline surface and the molecular adsorbates leading to a small charge transfer from the surface into the molecular layer. Therefore, we propose that the quasicrystalline order of the molecular adsorbate layer is the result of the quasicrystalline order of the surface itself that is imprinted onto the adsorbate layer by partial chemical interaction (weak chemisorption) between the molecular adsorbates and the quasicrystalline surface. Tuning the molecule–surface interaction in such systems hence opens a new way to design quasicrystalline order in a manifold of functional molecular materials on quasicrystalline surfaces.

Acknowledgments

The work was funded by the Deutsche Forschungsgemeinschaft (DFG, German Research Foundation)—TRR 173-268565370 (Project B05). MM acknowledges support by the Carl-Zeiss Stiftung for a post-doctoral fellowship. We thank Johannes Stöckl and Benito Arnoldi for fruitful discussions and their help during the preparation of data analysis script and the ARPES data acquisition. DLS and TAL. acknowledge support by the Office of Science, Basic Energy Sciences, Materials Sciences, and Engineering Division of the US Department of Energy (USDOE), under Contract No. DE-AC02-07CH11358 with the US Department of Energy.

ORCID iDs

M Maniraj https://orcid.org/0000-0001-7305-1368
S R Barman https://orcid.org/0000-0002-2517-6286
S Mathias https://orcid.org/0000-0002-1255-521X
B Stadtmüller https://orcid.org/0000-0001-8439-434X

References

[1] Shechtman D, Blech I, Gratias D and Cahn J W 1984 *Phys. Rev. Lett.* **53** 1951
[2] Stadnik Z M (ed) 1999 *Physical Properties of Quasicrystals* (Berlin: Springer)
[3] Steurer W and Deloudi S 2009 *Crystallography of Quasicrystals: Concepts, Methods and Structures* (Berlin: Springer)
[4] Bindi L, Steinhardt P J, Yao N and Lu P J 2009 *Science* **324** 1306
[5] Steinhardt P J and Bindi L 2012 *Rep. Prog. Phys.* **75** 092601
[6] Förster S, Meinel K, Hammer R, Trautmann M and Widdra W 2013 *Nature* **502** 215

[7] Iacovella C R, Keys A S and Glotzer S C 2011 *Proc. Natl Acad. Sci.* **108** 20935
[8] Ahn S J *et al* 2018 *Science* **361** 782–6
[9] Yao W *et al* 2018 *Proc. Natl Acad. Sci.* **115** 6928–33
[10] Franke K J, Sharma H R, Theis W, Gille P, Ebert P and Rieder K H 2002 *Phys. Rev. Lett.* **89** 156104
[11] Sharma H R *et al* 2013 *Nat. Commun* **4**
[12] Ledieu J, Leung L, Wearing L H, McGrath R, Lograsso T A, Wu D and Fournée V 2008 *Phys. Rev.* B **77** 073409
[13] Ledieu J, Hoeft J T, Reid D E, Smerdon J A, Diehl R D, Ferralis N, Lograsso T A, Ross A R and McGrath R 2005 *Phys. Rev.* B **72** 035420
[14] Sharma H R, Fournée V, Shimoda M, Ross A R, Lograsso T A, Gille P and Tsai A P 2008 *Phys. Rev.* B **78** 155416
[15] Sharma H R, Shimoda M, Ross A R, Lograsso T A and Tsai A P 2005 *Phys. Rev.* B **72** 045428
[16] Krajčí M, Hafner J, Ledieu J, Fournée V and McGrath R 2010 *Phys. Rev.* B **82** 085417
[17] Shukla A K, Dhaka R S, Biswas C, Banik S, Barman S R, Horn K, Ebert P and Urban K 2006 *Phys. Rev.* B **73** 054432
[18] Shukla A K *et al* 2009 *J. Phys.: Condens. Matter* **21** 405005
[19] Ledieu J, Krajčí M, Hafner J, Leung L, Wearing L H, McGrath R, Lograsso T A, Wu D and Fournée V 2009 *Phys. Rev.* B **79** 165430
[20] Singh V K *et al* 2020 *Phys. Rev. Res.* **2** 013023
[21] Maniraj M, Rai A, Barman S R, Krajčí M, Schlagel D L, Lograsso T A and Horn K 2014 *Phys. Rev.* B **90** 115407
[22] Fournée V, Gaudry É, Ledieu J, de Weerd M-C, Wu D and Lograsso T 2014 *ACS Nano* **8** 3646
[23] Smerdon J A *et al* 2014 *Nano Lett.* **14** 1184
[24] Kalashnyk N, Ledieu J, Gaudry É, Cui C, Tsai A-P and Fournée V 2018 *Nano Res.* **11** 2129
[25] Ledieu J, Muryn C A, Thornton G, Diehl R D, Lograsso T A, Delaney D W and McGrath R 2001 *Surf. Sci.* **472** 89
[26] Zollner E M, Schenk S, Förster S and Widdra W 2019 *Phys. Rev.* B **100** 205414
[27] Altman E I and Colton R J 1993 *Phys. Rev.* B **48** 18244
[28] Bauert T, Merz L, Bandera D, Parschau M, Siegel J S and Ernst K-H 2009 *J. Am. Chem. Soc.* **131** 3460
[29] France C B, Schroeder P G, Forsythe J C and Parkinson B A 2003 *Langmuir* **19** 1274
[30] Haag N *et al* 2020 *Phys. Rev.* B **101** 165422
[31] Wießner M, Rodríguez Lastra N S, Ziroff J, Forster F, Puschnig P, Dössel L, Müllen K, Schöll A and Reinert F 2012 *New J. Phys.* **14** 113008
[32] Wang S, Tan L Z, Wang W, Louie S G and Lin N 2014 *Phys. Rev. Lett.* **113** 196803
[33] Kwon S and Choi W K 2015 *Sci. Rep.* **5** 17834
[34] Puschnig P and Lüftner D 2015 *J. Electron Spectrosc. Relat. Phenom.* **200** 193
[35] Udhardt C, Otto F, Huempfner T, Schröter B, Forker R and Fritz T 2018 *J. Electron Spectrosc. Relat. Phenom.* **227** 40
[36] Maniraj M *et al* 2019 *Commun. Phys.* **2** 12
[37] Horcas I, Fernández R, Gómez-Rodríguez J M, Colchero J, Gómez-Herrero J and Baro A M 2007 *Rev. Sci. Instrum.* **78** 013705
[38] Nečas D and Klapetek P 2011 *Open Phys.* **10** 181
[39] Shukla A K *et al* 2009 *Phys. Rev.* B **79** 134206
[40] Martínez-Blanco J, Klingsporn M and Horn K 2010 *Surf. Sci.* **604** 523
[41] Wang B, Ma X, Caffio M, Schaub R and Li W-X 2011 *Nano Lett.* **11** 424
[42] Huempfner T, Sojka F, Forker R and Fritz T 2015 *Surf. Sci.* **639** 80
[43] Penrose R 1979 *Math. Intel.* **2** 32
[44] Krajčí M, Hafner J, Ledieu J and McGrath R 2006 *Phys. Rev.* B **73** 024202
[45] Krajčí M and Hafner J 2008 *Phys. Rev.* B **77** 134202
[46] Levine D 1986 *J. Phys. Colloques* **47** C3–125
[47] Neuhold G, Barman S R, Horn K, Theis W, Ebert P and Urban K 1998 *Phys. Rev.* B **58** 734
[48] Nayak J *et al* 2012 *Phys. Rev. Lett.* **109** 216403
[49] Stadnik Z M, Purdie D, Baer Y and Lograsso T A 2001 *Phys. Rev.* B **64** 214202
[50] Puschnig P *et al* 2009 *Science* **326** 702
[51] Willenbockel M *et al* 2013 *New J. Phys.* **15** 033017
[52] Jansen M *et al* 2020 *New J. Phys.* **22** 063012
[53] Curcio D, Omiciuolo L, Pozzo M, Lacovig P, Lizzit S, Jabeen N, Petaccia L, Alfè D and Baraldi A 2016 *J. Am. Chem. Soc.* **138** 3395
[54] Barman S R *et al* 2017 arXiv:1704.06783v1 [Cond-Mat]
[55] Zou Y, Kilian L, Schöll A, Schmidt T, Fink R and Umbach E 2006 *Surf. Sci.* **600** 1240
[56] Duhm S, Gerlach A, Salzmann I, Bröker B, Johnson R L, Schreiber F and Koch N 2008 *Org. Electron.* **9** 111
[57] Tamai A, Seitsonen A P, Baumberger F, Hengsberger M, Shen Z-X, Greber T and Osterwalder J 2008 *Phys. Rev.* B **77** 075134
[58] Methfessel T, Steil S, Baadji N, Großmann N, Koffler K, Sanvito S, Aeschlimann M, Cinchetti M and Elmers H J 2011 *Phys. Rev.* B **84** 224403
[59] Steil S *et al* 2013 *Nat. Phys.* **9** 242
[60] Willenbockel M, Lüftner D, Stadtmüller B, Koller G, Kumpf C, Soubatch S, Puschnig P, Ramsey M G and Tautz F S 2015 *Phys. Chem. Chem. Phys.* **17** 1530
[61] Armbrust N, Schiller F, Güdde J and Höfer U 2017 *Sci. Rep.* **7** 46561
[62] Graus M, Grimm M, Metzger C, Dauth M, Tusche C, Kirschner J, Kümmel S, Schöll A and Reinert F 2016 *Phys. Rev. Lett.* **116** 147601